Asian Journal of Chemistry; Vol. 36, No. 12 (2024), 2790-2800

ASIAN JOURNAL OF CHEMISTRY

https://doi.org/10.14233/ajchem.2024.32598

PPARγ and COX1 Inhibition of Linoleic Acid as Potential Bioactive Molecule in Aqueous Extract of *Tinospora cordifolia* (Wild.): A *in silico* based Approach

BISWABARA ROY[1,2,*], SANDIP SEN[1], D. SENTHIL KUMAR[2] and N. KANNAPPAN[2]

[1]School of Pharmacy, Guru Nanak Institutions Technical Campus, Khanapur, Ibrahimpatnam-501506, India
[2]Department of Pharmacy, Faculty of Engineering & Technology, Annamalai University, Annamalai Nagar-608002, India

*Corresponding author: E-mail: bishwabara1980@gmail.com

Received: 19 August 2024; *Accepted*: 17 October 2024; *Published online*: 30 November 2024; AJC-21819

In this work, the ethyl acetate extract of *Tinospora cardifolia* was analyzed using GC-MS and phytochemical analysis. The FTIR analysis and UV spectroscopy were used to further validate the structures of the isolated compounds. For the selected compounds, the computational methods were used to conduct an *in silico* analysis on their molecular, physico-chemical and druglikeliness properties. Moreover, the pharmacokinetic profile and additional toxicity potential were ascertained. Swiss ADME tools and OSIRIS data warrior were used in the investigation. The docking experiment was used to examine the anti-inflammatory and antidiabetic characteristics. The α-glucosidase, peroxisome proliferator-activated receptor, glucose transporter-1 and cyclooxygenases 1 and 2 were targeted for inhibition. Approximately 23 chemicals were found during GC-MS analysis. Each of the compounds have shown the pharmacokinetic potential and moderate to good drug likeliness. The compounds bioactivity score against enzyme receptors was high. The least harmful profile of PGP and CYP inhibitory actions was indicated by the ADMET prediction. Linoleic acid (molecule-12) has a strong binding affinity for PPARγ and COX1 targeted proteins under inquiry as demonstrated by the docking studies.

Keywords: *Tinospora cordifolia,* Gas chromatography, *In silico* study, Molecular docking, PPARγ, Cyclooxygenasse-1.

INTRODUCTION

India is rich in biodiversity, particularly in medicinal plants. Among these, *Tinospora cordifolia* stands out for its diverse bioactive compounds and proven medicinal significance. Despite its importance, this plant has not received the scientific attention it deserves. A wide variety of plants are utilized in medicine for therapeutic or preventive purposes [1]. The healing properties of these medicinal plants are due to the presence of active compounds such as alkaloids, flavonoids, glycosides, vitamins, tannins and coumarins. These natural substances have physiological effects on the human body, interact with pathogens and inhibit their growth at various stages, ultimately helping to prevent and cure diseases [2].

Tinospora cordifolia (Wild.) Miers ex Hook. F. and Thoms, a member of the Menispermaceae family, is a large, deciduous, climbing shrub widely distributed across India, particularly in tropical regions up to an altitude of 300 m [3]. This plant is commonly known as the heart-leaved Moonseed in English, Guduchi in Sanskrit and Giloy in Hindi. *T. cordifolia* is a highly valued medicinal plant in Ayurveda, known for its role in preventing and treating various human ailments. Due to its rich content of diverse phytochemicals, Giloy is widely used in pharmaceutical chemistry for its anti-osteoporotic, hepatoprotective, immunomodulatory, antihyperglycemic, anti-tumor and anti-HIV properties [4].

Type 2 diabetes, a multifaceted disorder frequently associated with genetic predispositions, is significantly more prevalent than type 1 diabetes, with an incidence rate approximately 20 times higher. The risk of developing type 2 diabetes is exacerbated by suboptimal lifestyle choices and unregulated dietary habits, which often lead to overweight and obesity, particularly as individuals age [5]. The interrelation between type 2 diabetes and arthritis is underscored by the convergence of common risk factors, with nearly 48% of individuals diagnosed with type 2 diabetes also experiencing arthritis. Aging emerges as a critical

determinant for both conditions, necessitating a range of therapeutic interventions to effectively manage the complexities of diabetes and arthritis [6].

Structure-based drug design (SBDD) and *in silico* methods play a crucial role in optimizing natural products as therapeutic agents. These approaches leverage the complex structures of natural compounds and detailed three-dimensional target data to enhance drug efficacy and specificity [7]. By predicting interactions between natural products and biological targets, *in silico* studies streamline the drug discovery process. However, the success of these techniques depends on accurate structural data and robust computational models, requiring careful integration with experimental validation due to the complexity of natural products [8].

The present study focused on designing compounds from the aqueous extract of *Tinospora cardifolia* using web-based and software-based techniques, including SBDD (structure-based drug design), FBDD (fragment-based drug design) and LBDD (ligand-based drug design). Initial identification of these compounds was carried out through spectral analysis and GC-MS. Based on existing literature, the study also aimed to identify specific binding proteins associated with the anti-diabetic and anti-inflammatory activities of the compounds.

EXPERIMENTAL

Plant extract and phytochemical analysis: The fresh stem of plant was collected from Siddipet (Location coordinates: 18.1ºN 78.85ºE). The samples was authenticated from Botany Department, Satavahana University, with apecimen accession No.: ENM-100129. The stems was air dried in shades at room temperature and then grinded to coarse powder using mixer grinder (instrument: Premier Wonder Wet Grinder Pg 503). The stem powder was collected in muslin begs having mash size 200 and then transferred to the Soxhlet apparatus. The extraction was carried out with petroleum ether and continued the process until colourless liquid was obtained. Dried the residue in muslin bag and repeat the process with water until colourless liquid was obtained. The collected extract was concentrated in the rotary flash evaporation fitted with vacuum pump at 100 ºC at a pressure of 2 dynes/cm^2 at 100 rpm and finally stored the residue in Ambered colour glass container. The aqueous extract was subjected to phytochemical analysis as per literature procedure.

GC-MS analysis: The procedure involved first dissolving 100 mg of the extract in 100 mL of HPLC-grade methanol, then diluting the solution to a concentration of 30 µg/mL. Gas chromatography (GC) analysis was performed using an Agilent 7890A GC System with an HP5 column (30 m × 0.25 mm × 0.25 µm) and helium as the carrier gas at a flow rate of 1 mL/min. The oven temperature was set to 280 °C and a 1 µL sample was injected at 70 ºC with a split ratio of 1:10, with a total run time of 50 min. For mass spectrometry (MS), the JEOL AccuTOF GCv/JMS-T100GCv was utilized with electron ionization (EI) in positive mode, covering a mass range of 35 to 800 amu. The ion source was maintained at 220 ºC, with a solvent delay of 4 min and the total MS run time was 50 min. Compounds were identified by comparing their mass spectra to the NIST library and their concentrations were determined based on peak areas using the following formula:

$$\text{Compound (\%)} = \frac{\text{Peak area at respective retention time}}{\text{Total peak area}} \times 100$$

Determination of wavelength by UV-spectroscopic method: Aqueous extract (100 mg) was transferred to a 100 mL volumetric flask and diluted with 100 mL of phosphate buffer (pH 6.8). About 10 mL of aforementioned solution, dilute it with diluents to volume and thoroughly mix (concentration: 100 µg/mL) in a 100 mL volumetric flask. To get the required concentration of 30 µg/mL for analysis, 3 mL of stock solutions were obtained and added to a 10 mL volumetric flask. The absorbance was measured by scanning the solution in spectrum mode between 200 and 400 nm.

FTIR analysis: FTIR analysis was carried out using the Bruker 3000 Hyperion Microscope coupled with the Vertex 80 FTIR System, incorporating Micro ATR and Grazing Angle accessories. Approximately 1 mg of extract was placed on the sampling plate and the scan was performed over the 4000-450 cm^{-1} range with a spectral resolution of 0.2 cm^{-1}.

Structure preparation: The structural representation of the target compound was meticulously constructed using ChemDraw Ultra 12.0.2. SMILES notations were generated through ACD Labs ChemSketch version 12.0 and subsequently converted to mol2 format using Chem3D Pro 12, facilitating further structural analysis and modeling.

***In silico* study:** The SMILES notation was used to carried out to determine *in silico* study. The Osiris DataWarrior software to calculate molecular, physico-chemical properties and toxicity potential. Fraction C*sp*^{3} and molar refractive index were determined using the SwissADME online tool. The absorption percentage (% Abs) was calculated using the following formula:

$$\%\text{Abs} = 109 - (0.345 \times \text{TPSA})$$

The SwissADME tool was used to predict drug-likeness properties, pharmacokinetic potential and bioavailability score. Molinspiration software version 2011.06 was used to calculate scores for drug targets such as enzymes, nuclear receptors, kinase inhibitors, GPCR ligands and ion channel modulators. The bioactivity radar charts for the molecules and standards were prepared using the SwissADME tool. A boiled egg diagram was created to visualize these results using the SwissADME tool [9].

Docking analysis: SwissDock and UCSF Chimera 1.5.3 were used for the docking study to perform interactive visualization and analysis of molecular structures, including sequence alignments, density maps and trajectories. Human PPARγ ligand binding domain complexed with rosiglitazone (5YCP), human glucose transporter GLUT1 (4PYP), COX-1 complexed with Ibuprofen (1EQG) and COX-2 active site complexed with celecoxib (3LN1) were the target proteins that were retrieved in PDB format from the RCSB protein data bank. The SwissDock server was used to perform flexible docking once the molecules were converted to mol2 format. UCSF Chimera 1.5.3 was used to examine the binding score, posture and residues. Out of 250 clusters, the best binding score was chosen.

RESULTS AND DISCUSSION

Phytochemical studies: The aqueous extract had a yield of 44.1%. The phytochemical results showed the presence of alkaloids, steroids, flavonoids, phenol, carbohydrates, terpenoids and aliphatic chemicals are abundant in the aqueous extract.

GC-MS analysis: Fig. 1 showed the full scan GC-MS analysis results and 23 compounds (Fig. 2) was found in the aqueous extracts. The data for chromatographic analysis is represented in Table-1. The NIST search library, prepared during the study, was utilized to validate the structures of the molecules in extracts. Molecule TCA 12 (8.58%) was found in the highest concentration at the retention time of 23.84 min and was traced in the aqueous extract.

Molecular property: The molecular shape, flexibility and complexity play significant roles in drug action and binding affinity to receptor molecules. Linear-form molecules generally exhibited good therapeutic potential [10]. For strong binding affinity towards receptors, high flexibility and low complexity of molecules are considered [11,12]. For aqueous extract, the molecular properties are depicted in Table-2. Molecules TCA 3, TCA 6, TCA 7, TCA 11, TCA 14, TCA 15 and TCA 20 are

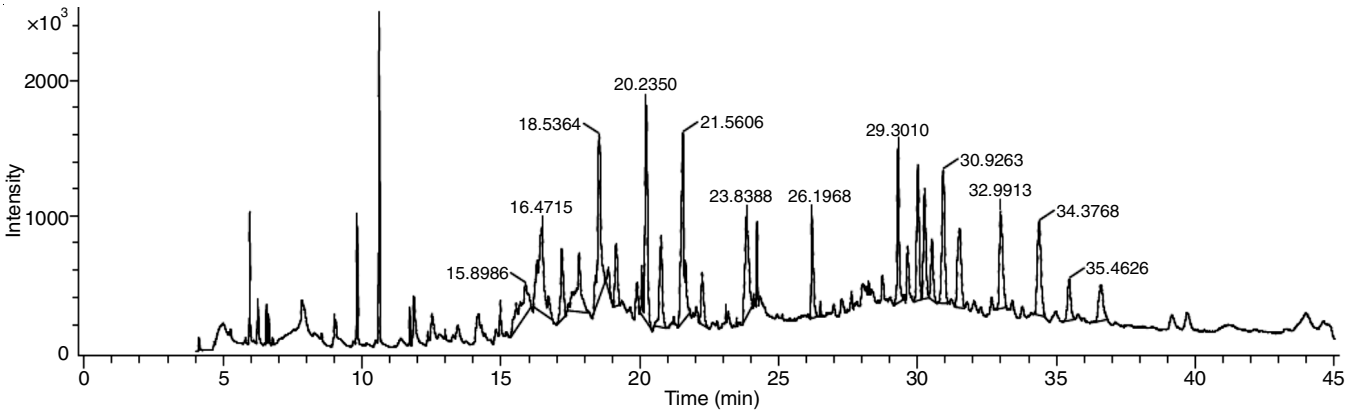

Fig. 1. Gas chromatogram of aqueous extract of *Tinospora cordifolia* (Wild.)

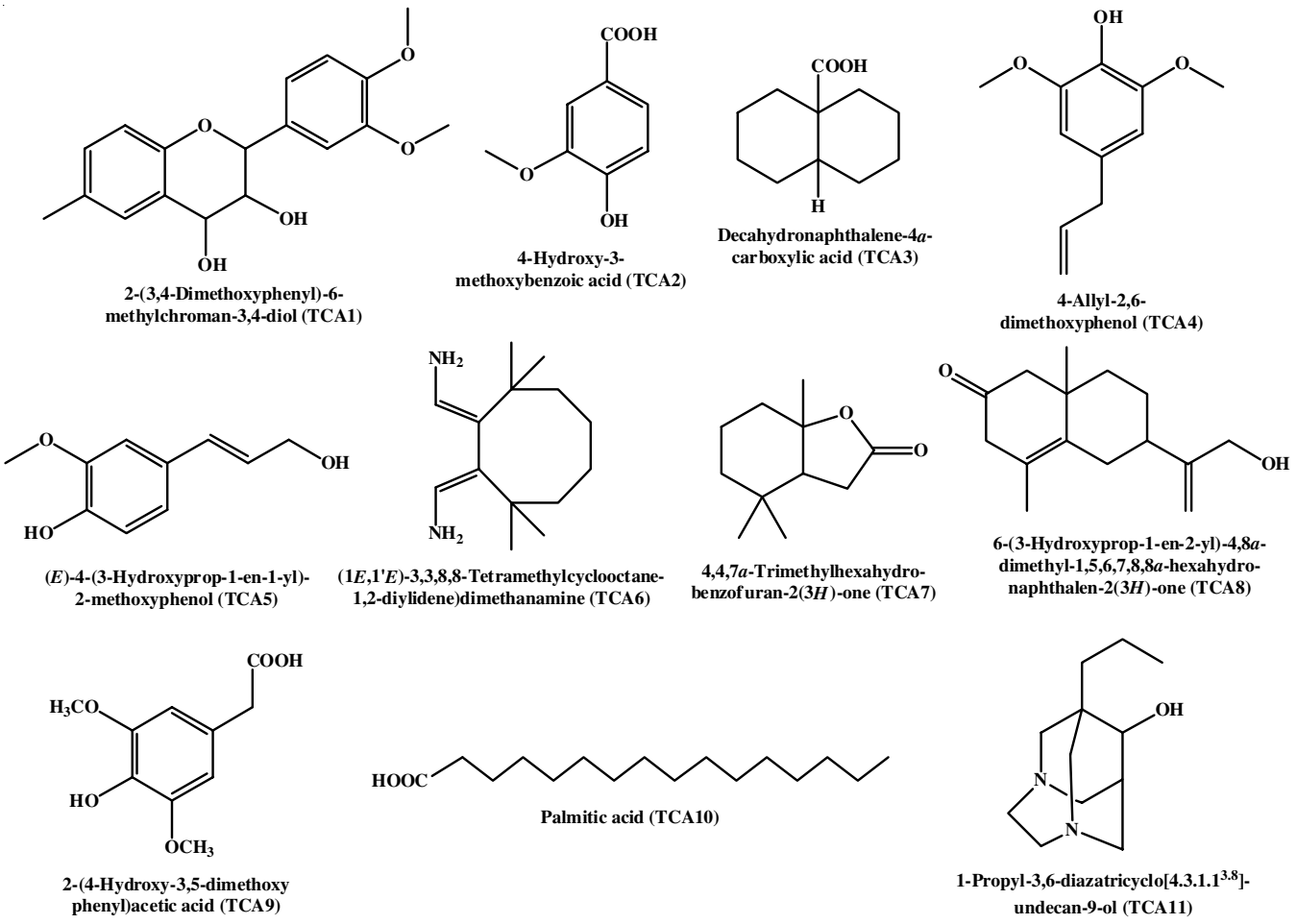

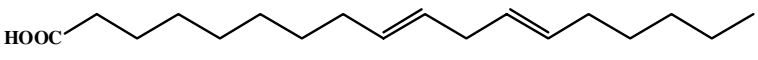

(9*E*,12*E*)-Octadeca-9,12-dienoic acid (TCA12)

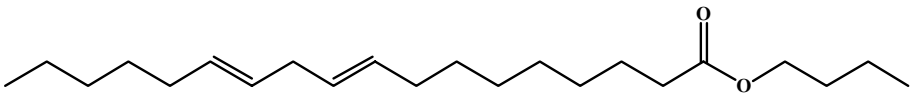

(9*E*,12*E*)-Butyl octadeca-9,12-dienoate (TCA13)

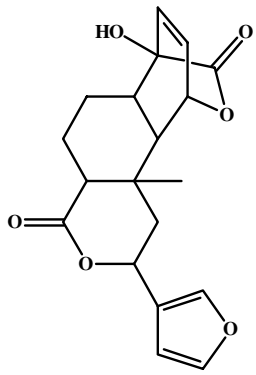

(10*S*)-2-(Furan-3-yl)-7-hydroxy-10*b*-methyl-4*a*,5,6,6*a*-7,10,10*a*,10*b*-octahydro-1*H*-10,7-(epoxymethano)benzo[*f*]isochromene-4,12(2*H*)-dione (TCA14)

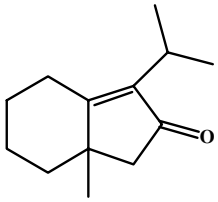

3-Isopropyl-7*a*-methyl-5,6-7,7*a*-tetrahydro-1*H*-inden-2(4*H*)-one (TCA15)

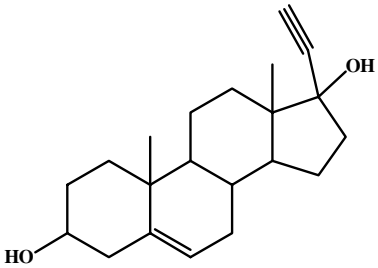

17-Ethynyl-10,13-dimethyl-2,3,4,7,8,9,10,11,12,13,1,15,16,17-tetradecahydro-1*H*-cyclopenta[*a*]phenanthrene-3,17-diol (TCA16)

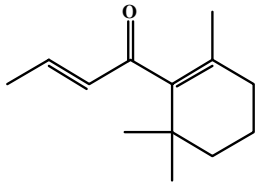

(*E*)-1-(2,6,6-Trimethylcyclohex-1-en-1-yl)but-2-en-1-one (TCA18)

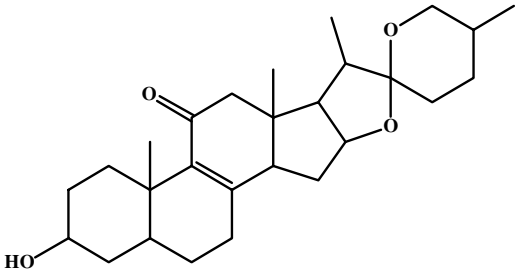

4-Hydroxy-5',6*a*,8*a*,9-tetramethyl-octadecahydrospiro-[naphtha[2',1':4,5]indeno[2,1-*b*]furan-10,2'-pyran]-7(11*aH*)-one (TCA17)

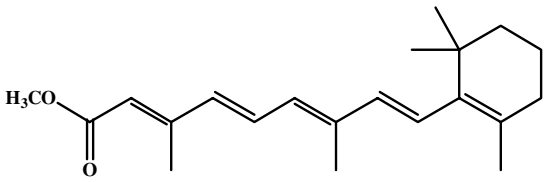

(2*E*,4*E*,6*E*,8*E*)-Methyl 3,7-dimethyl-9-(2,6,6-trimethylcyclohex-1-en-1-yl)nona-2,4,6,8-tetraenoate (TCA19)

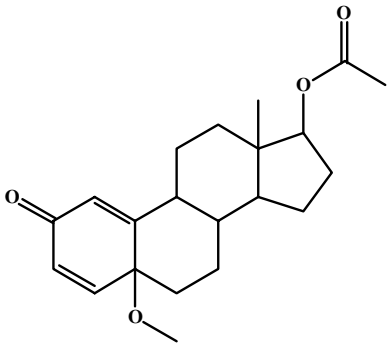

5-Methoxy-13-methyl-2-oxo-5,6,7,8,9,11,12,13,14,15,16,17-dodecahydro-2*H*-cyclopenta[*a*]-phenanthren-17-yl acetate (TCA20)

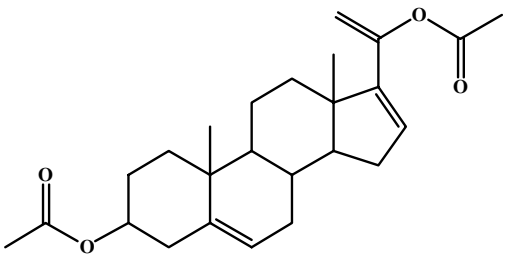

1-(3-Acetoxy-10,13-dimethyl-2,3,4,7,8,9,10,11,12,13,14,15-dodecahydro-1*H*-cyclopenta[*a*]phenanthren-17-yl)vinyl acetate (TCA21)

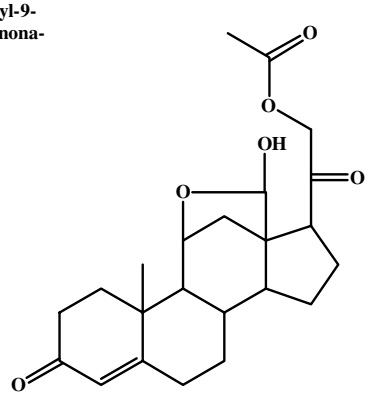

2-(3-Hydroxy-12*a*-methyl-10-oxo-1,3,4,5,6,6*a*,6*b*,7,8,10,11,12,12*a*,12*b*-tetradecahydro-1,3*a*-methanocyclopenta[*c*]naphtha[2,1-*e*]oxepin-4-yl)-2-oxoethyl acetate (TCA22)

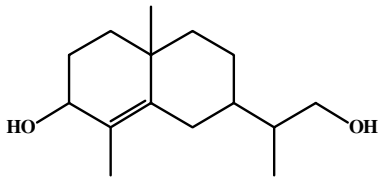

7-(1-Hydroxypropan-2-yl)-1,4*a*-dimethyl-2,3,4,4*a*,5,6,7,8-octahydronaphthalen-2-ol (TCA23)

Fig. 2. Structures of some compounds identified in aqueous extract of aqueous extract of *Tinospora cordifolia* (Wild.)

TABLE-1
GC-MS ANALYSIS FOR AQUEOUS EXTRACT OF *Tinospora cordifolia* (Wild.)

Peak No.	Time (min)	Peak area (%)	m.w.	m.f.	Probability (%)
1	15.90	4.32	316.00	$C_{18}H_{20}O_5$	23.70
2	16.47	7.85	168.00	$C_8H_8O_4$	50.30
3	17.20	2.81	182.00	$C_{11}H_{18}O_3$	12.40
4	17.82	4.46	194.00	$C_{11}H_{14}O_3$	37.60
5	18.54	7.47	180.00	$C_{10}H_{12}O_3$	72.40
6	18.88	0.82	210.00	$C_{11}H_{22}N_4$	11.40
7	19.15	2.27	182.00	$C_{11}H_{18}O_2$	11.30
8	20.24	2.90	234.00	$C_{15}H_{22}O_2$	25.80
9	20.77	3.69	212.00	$C_{10}H_{12}O_5$	12.60
10	21.56	5.48	256.00	$C_{16}H_{32}O_2$	56.80
11	22.25	1.95	210.00	$C_{12}H_{22}N_2O$	15.70
12	23.84	8.58	290.00	$C_{18}H_{32}O_2$	19.20
13	26.20	8.37	336.00	$C_{22}H_{40}O_2$	40.80
14	29.30	4.64	358.00	$C_{20}H_{22}O_6$	63.90
15	30.02	4.59	192.00	$C_{13}H_{20}O$	21.40
16	30.26	3.71	314.00	$C_{21}H_{30}O_2$	20.50
17	30.52	2.11	428.00	$C_{27}H_{40}O_4$	41.50
18	30.93	5.52	192.00	$C_{13}H_{20}O$	9.52
19	31.51	4.25	314.00	$C_{21}H_{30}O_2$	14.00
20	32.99	4.73	344.00	$C_{21}H_{28}O_4$	16.30
21	34.38	5.14	398.00	$C_{25}H_{34}O_4$	19.80
22	35.46	1.94	402.00	$C_{23}H_{30}O_6$	9.89
23	36.60	2.41	238.00	$C_{15}H_{26}O_2$	7.21

TABLE-2
MOLECULAR PROPERTIES OF SOME MOLECULES ISOLATED FROM AQUEOUS EXTRACT OF *T. cordifolia*

Molecule	Shape index[a]	Molecular flexibility[b]	Molecular complexity[b]
TCA1	0.56	0.31	0.85
TCA2	0.58	0.28	0.65
TCA3	0.46	0.51	0.60
TCA4	0.57	0.39	0.67
TCA5	0.69	0.39	0.66
TCA6	0.43	0.38	0.68
TCA7	0.46	0.25	0.70
TCA8	0.58	0.49	0.79
TCA9	0.53	0.47	0.64
TCA10	0.94	0.52	0.35
TCA11	0.46	0.51	0.73
TCA12	0.95	0.60	0.37
TCA13	0.95	0.59	0.44
TCA14	0.44	0.37	0.96
TCA15	0.50	0.35	0.77
TCA16	0.52	0.31	0.89
TCA17	0.51	0.30	1.00
TCA18	0.57	0.46	0.66
TCA19	0.68	0.31	0.64
TCA20	0.48	0.36	0.91
TCA21	0.55	0.37	0.91
TCA22	0.51	0.36	0.99
TCA23	0.52	0.48	0.77

[a]Molecular shape index (spherical = 0.5 = linear), [b]Molecular flexibility (low = 0.5 = high), [c]Molecular complexity (low = 0.5 = high)

spherical, while the molecules TCA 3, TCA 10, TCA 11, TCA 12 and TCA 13 have high molecular flexibility. The molecules TCA 10, TCA 12 and TCA 13 bear low complexity.

Physico-chemical properties: The physico-chemical properties of molecules such as molecular weight, solubility, partition coefficient, H-acceptors, H-donors [13], total surface area, relative polar surface area, TPSA (Å^2) [14], percentage of absorption, fraction Csp^3 and molar refractive index [15] have a significant impact on their biological activity and druglikeness. The physico-chemical properties of aqueous extract are shown in Table-3.

TABLE-3
PHYSICO-CHEMICAL PROPERTIES OF SOME MOLECULES ISOLATED FROM AQUEOUS EXTRACT OF *T. cordifolia*

Molecules	m.w.	cLogP	cLogS	Solubility	H-acceptors	H-donors	Fraction Csp^3	MR	Total surface area	Relative PSA	TPSA[e] (Å^2)	Abs. (%)
TCA1	316.3	2.4	-2.7	Moderately soluble	5	2	0.33	85.35	236.5	0.23	68.1	85.4
TCA2	168.1	0.7	-1.3	Soluble	4	2	0.12	41.92	125.9	0.39	66.7	85.9
TCA3	182.2	2.0	-2.7	Soluble	2	1	0.91	52.27	143.5	0.18	37.3	96.1
TCA4	194.2	2.2	-2.0	Soluble	3	1	0.27	55.55	162.4	0.20	38.6	95.6
TCA5	180.2	1.4	-1.7	Soluble	3	2	0.20	51.02	148.4	0.24	49.6	91.8
TCA6	222.4	3.2	-3.1	Soluble	2	2	0.71	71.24	191.3	0.15	52.0	91.0
TCA7	182.3	1.8	-2.5	Soluble	2	0	0.91	51.83	139.3	0.16	26.3	99.9
TCA8	234.3	3.1	-2.7	Soluble	2	1	0.67	70.14	186.2	0.14	37.3	96.1
TCA9	212.2	0.6	-1.3	Soluble	5	2	0.30	52.99	161.9	0.36	75.9	82.7
TCA10	256.4	6.0	-4.2	Moderately soluble	2	1	0.94	80.80	242.5	0.10	37.3	96.1
TCA11	210.3	0.9	-0.5	Soluble	3	1	1.0	67.98	157.7	0.12	26.7	99.7
TCA12	280.4	6.4	-4.3	Poorly soluble	2	1	0.72	89.46	267.9	0.09	37.3	96.1
TCA13	336.5	8.2	-5.2	Poorly soluble	2	0	0.77	108.20	325.1	0.07	26.3	99.9
TCA14	344.3	0.6	-3.1	Soluble	6	1	0.58	85.55	234.1	0.31	85.9	79.3
TCA15	192.3	3.2	-2.9	Soluble	1	0	0.77	59.84	155.6	0.08	17.0	103.1
TCA16	314.4	3.2	-4.4	Soluble	2	2	0.81	94.13	236.5	0.11	40.4	95.0
TCA17	428.6	4.3	-5.1	Moderately soluble	4	1	0.89	121.70	304.8	0.15	55.7	89.7
TCA18	192.3	3.3	-2.7	Soluble	1	0	0.62	61.48	167.9	0.07	17.0	103.1
TCA19	300.4	5.6	-3.4	Poorly soluble	2	0	0.45	94.80	267.8	0.08	26.3	99.9
TCA20	344.4	2.9	-3.7	Soluble	4	0	0.71	96.01	256.3	0.17	52.6	90.8
TCA21	398.5	5.4	-5.2	Moderately soluble	4	0	0.68	114.40	303.3	0.15	52.6	90.8
TCA22	402.4	2.0	-3.8	Soluble	6	1	0.78	105.00	280.7	0.25	89.9	77.9
TCA23	238.3	2.8	-2.8	Soluble	2	2	0.87	71.58	189.3	0.13	40.4	95.0

Druglikeness: The druglikeness attributes of all compounds present in aqueous extracts, as shown in Table-4 have been evaluated using various criteria. These criteria encompass well-known rules and scores such as Lipinski, Ghose, Veber, Egan and Muegge rules and bioavailability scores [16]. For the aqueous extract molecules TCA 10, TCA 12 and TCA 13, violets have different drug likeliness rules. Molecules like TCA 19 and TCA 21 violate the Lipinski rule, whereas molecules TCA 17 violets the Veber rules. The violation of the Muegge rule was followed by molecules TCA2, TCA3, TCA4, TCA5, TCA7, TCA15, TCA18 and TCA19. The bioavailability index for all compounds was determined to be 0.55. Among them, molecules TCA11, TCA14, TCA16, TCA17, TCA20 and TCA22 displayed favourable drug-likeness values with scores of 1.58, 0.73, 1.51, 1.38, 1.58 and 2.03, respectively. These results demonstrated promising drug-likeness attributes.

Bioactivity scores: The bioactivity scores of the isolated compounds were evaluated against various targets, including GPCR ligands (G-protein coupled receptors), ion channel modulators, kinase inhibitors, nuclear receptor ligands, protease inhibitors and enzyme inhibitors. Each compound was assigned a bioactivity score. A bioactivity score higher than 0 indicates a strong effect, while a score between -0.5 and 0 is classified as moderate and a score below 0.5 signifies inactivity [17].

Table-5 present the bioactivity scores of various compounds obtained from aqueous extracts. All molecules except TCA2, TCA4, TCA5 and TCA8 demonstrated the bioactivity scores exceeding 0 with the aqueous extract. Fig. 3 depicts a bioactivity reader based on the molecular and physico-chemical properties. Concerning the distinct receptors, the hierarchy of receptor affinity can be ranked as follows: enzyme inhibitor > nuclear receptor > GPCR ligand > ion channel modulator > protease inhibitor > kinase inhibitor.

Toxicity potential: The mutagenic, tumorigenic, reproductive and irritating properties of the compounds were also investigated. Molecule TCA10 exhibited tumorigenic properties, while the the reproductive effect was found in molecule

TABLE-4
DRUG-LIKLINESS OF SOME MOLECULES ISOLATED FROM AQUEOUS EXTRACT OF *T. cordifolia*

Molecule	Drug-likeness	Lipinski	Ghose	Veber	Egan	Muegge	Bioavailability Score
TCA1	-0.3	Y	Y	Y	Y	Y	0.55
TCA2	-1.6	Y	Y	Y	Y	No; 1 violation: MW < 200	0.85
TCA3	-6.5	Y	Y	Y	Y	No; 1 violation: MW < 200	0.85
TCA4	-4.6	Y	Y	Y	Y	No; 1 violation: MW < 200	0.55
TCA5	-1.5	Y	Y	Y	Y	No; 1 violation: MW < 200	0.55
TCA6	-6.9	Y	Y	Y	Y	Y	0.55
TCA7	-8.5	Y	Y	Y	Y	No; 1 violation: MW < 200	0.55
TCA8	-3.5	Y	Y	Y	Y	Y	0.55
TCA9	-1.4	Y	Y	Y	Y	Y	0.56
TCA10	-25.2	No; 1 violation: MLOGP > 4.15	Y	No; 1 violation: Rotors > 10	Y	No; 1 violation: XLOGP3 > 5	0.85
TCA11	1.6	No; 0 violation	Y	Y	Y	Y	0.55
TCA12	-25.6	No; 1 violation: MLOGP > 4.15	No; 1 violation: WLOGP > 5.6	No; 1 violation: Rotors > 10	No; 1 violation: WLOGP > 5.88	No; 1 violation: XLOGP3 > 5	0.85
TCA13	-29.6	No; 1 violation: MLOGP > 4.15	No; 1 violation: WLOGP > 5.6	No; 1 violation: Rotors > 10	No; 1 violation: WLOGP > 5.88	No; 2 violations: XLOGP3 > 5, Rotors > 15	0.55
TCA14	0.7	Y	Y	Y	Y	Y	0.55
TCA15	-4.7	Y	Y	Y	Y	No; 2 violations: MW < 200, Heteroatoms < 2	0.55
TCA16	1.5	Y	Y	Y	Y	Y	0.55
TCA17	1.3	Y	N; 1 violation: #atoms > 70	Y	Y	Y	0.55
TCA18	-5.6	Y	Y	Y	Y	No; 2 violations: MW < 200, Heteroatoms < 2	0.55
TCA19	-10.3	No; 1 violation: MLOGP > 4.15	Y	Y	Y	No; 1 violation: XLOGP3 > 5	0.55
TCA20	1.5	Y	Y	Y	Y	Y	0.55
TCA21	-4.0	No; 1 violation: MLOGP > 4.15	Y	Y	Y	Y	0.55
TCA22	2.0	Y	Y	Y	Y	Y	0.55
TCA23	-2.8	Y	Y	Y	Y	Y	0.55

Y: N violation

TABLE-5
BIOACTIVITY SCORES OF SOME MOLECULES ISOLATED FROM AQUEOUS EXTRACT OF *T. cordifolia*

Molecules	GPCR ligand	Ion channel modulator	Kinase inhibitor	Nuclear receptor ligand	Protease inhibitor	Enzyme inhibitor
TCA1	0.2	-0.1	-0.0	0.2	0.0	0.2
TCA2	-0.8	-0.4	-1.0	-0.6	-1.1	-0.3
TCA3	-0.2	0.0	-1.1	0.1	-0.4	0.3
TCA4	-0.6	-0.2	-0.8	-0.6	-1.0	-0.2
TCA5	-0.5	-0.0	-0.7	-0.3	-1.0	-0.1
TCA6	-0.4	-0.1	-0.5	-0.1	-0.3	0.1
TCA7	-0.6	-0.2	-0.8	-0.3	-0.8	-0.3
TCA8	-0.4	-0.0	-0.9	0.4	-0.5	0.4
TCA9	-0.3	-0.0	-0.5	-0.1	-0.4	0.1
TCA10	0.0	0.1	-0.3	0.1	-0.0	0.2
TCA11	-0.1	0.1	-0.6	-0.2	-0.3	0.0
TCA12	0.3	0.2	-0.6	0.3	0.1	0.4
TCA13	0.2	0.1	-0.1	0.2	0.1	0.2
TCA14	0.5	-0.2	-0.3	0.6	-0.1	0.5
TCA15	-0.6	-0.1	-1.0	-0.2	-0.5	0.0
TCA16	0.2	-0.1	-0.4	1.2	-0.1	0.8
TCA17	-0.1	-0.2	-0.6	0.5	-0.1	0.5
TCA18	-0.8	-0.2	-1.5	0.2	-0.6	0.3
TCA19	-0.2	-0.0	-0.3	-0.8	-0.1	0.4
TCA20	0.2	0.1	-0.4	1.0	0.2	0.7
TCA21	0.0	-0.0	-0.6	0.7	0.0	0.6
TCA22	-0.0	-0.2	-0.9	0.5	0.0	0.5
TCA23	-0.1	-0.1	-0.5	0.7	-0.2	0.5

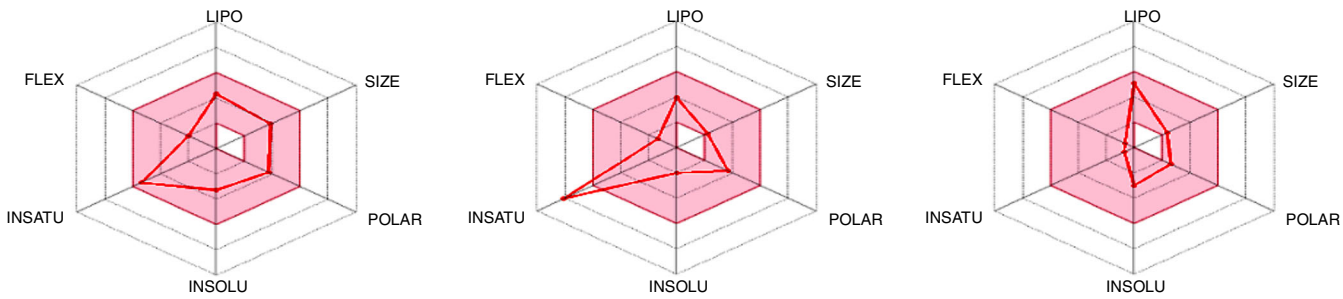

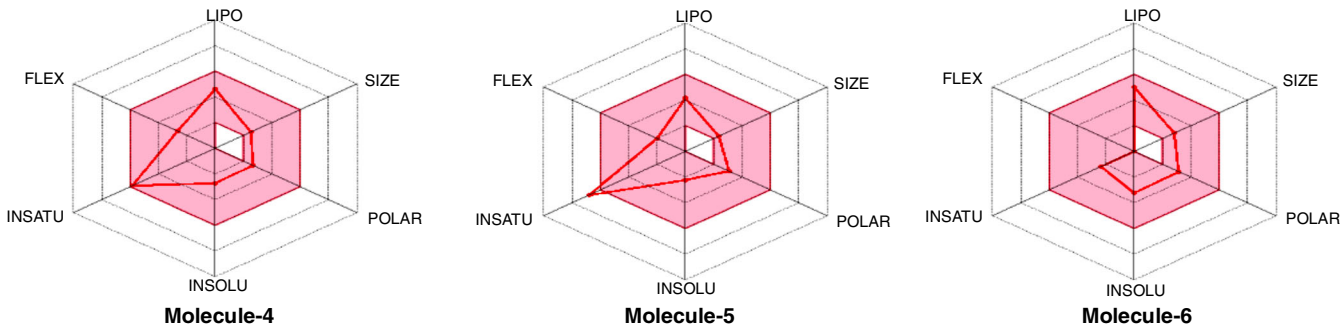

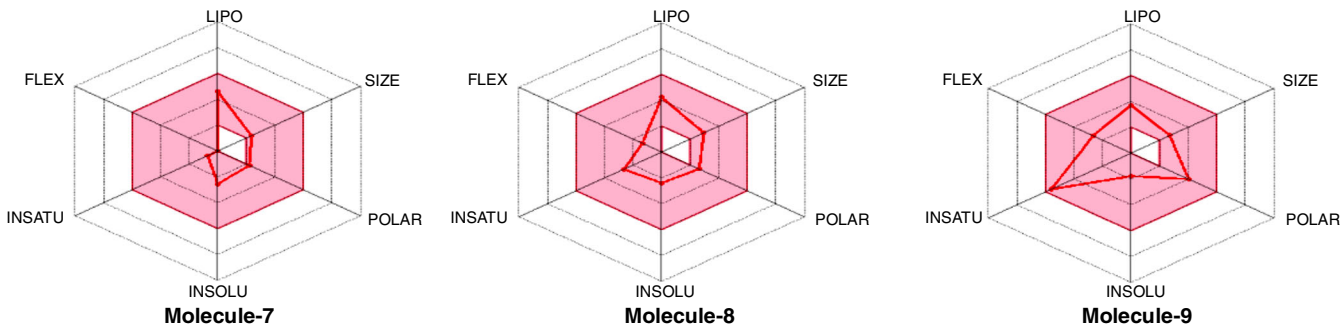

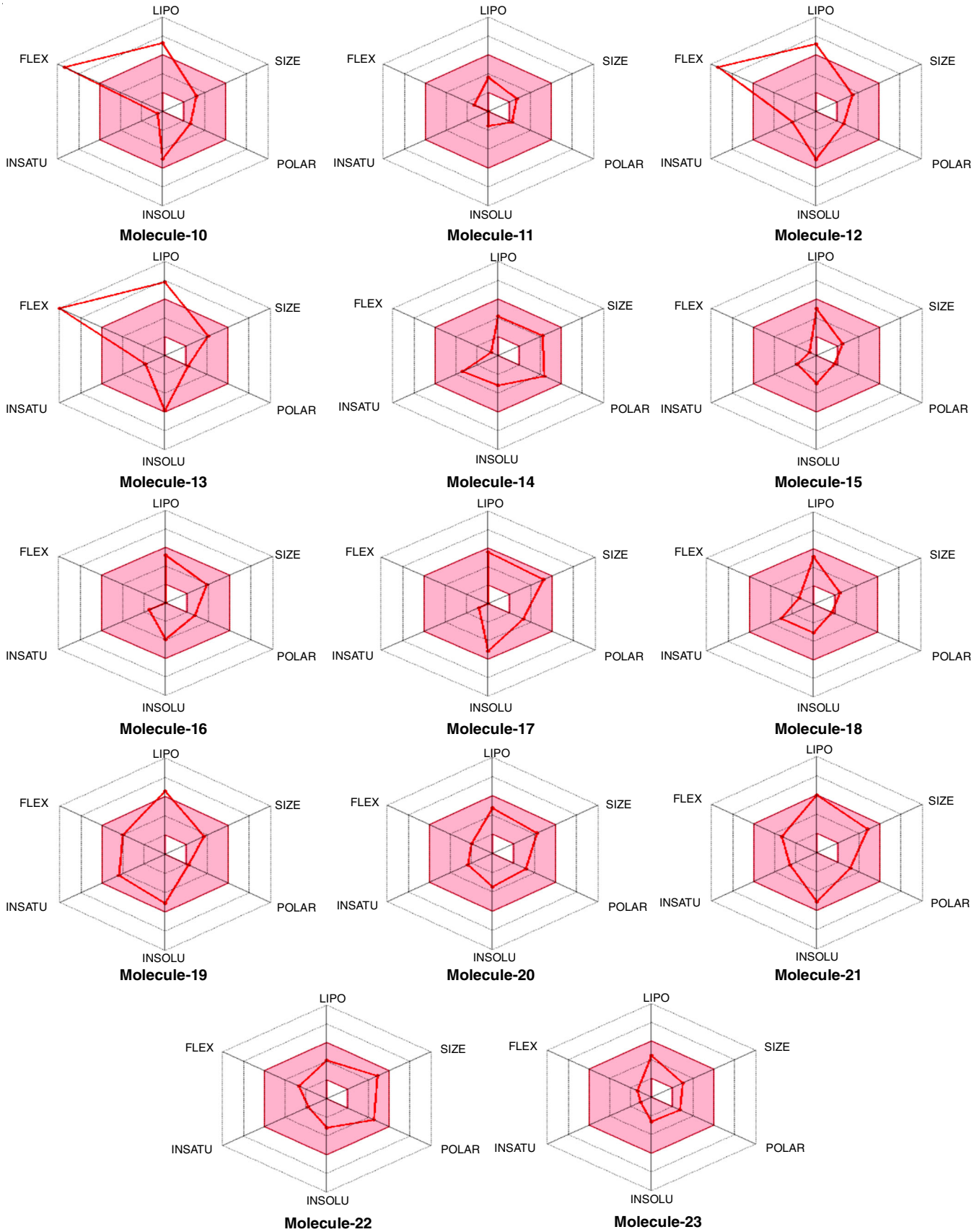

Fig. 3. Bioactvity rader of the molecules identified in aqueous extract [the coloured zone is suitable physico-chemical space for oral bioavailability. LIPO (Liphophilicity): 0.7 = XLOGP3 = +5.0; SIZE: 150 g/mol = MV; POLAR (Polarity): 20 Å^2 = TPSA = 130 Å^2; INSOLU (Insolubility): 0 = LOGS (ESOL) = 5.0; INSATU (Insaturation): 0.25 = Fraction Csp^3 = 1; FLEX (Flexibility): 0 = Number of rotatable bond = 9

TCA22. The most irritant behaviour was found for molecules TCA5, TCA10, TCA13, TCA14 and TCA19 (Table-6).

TABLE-6
TOXICITY POTENTIAL OF SOME MOLECULES ISOLATED FROM AQUEOUS EXTRACT OF *T. cordifolia*

Molecules	Mutagenic	Tumorigenic	Reproductive effective	Irritant
TCA1	–	–	–	–
TCA2	++	–	–	–
TCA3	–	–	–	–
TCA4	–	–	–	–
TCA5	–	–	–	++
TCA6	–	–	–	–
TCA7	–	–	–	–
TCA8	–	–	–	+
TCA9	–	–	–	–
TCA10	–	++	–	++
TCA11	–	–	–	–
TCA12	–	–	–	–
TCA13	–	–	–	++
TCA14	–	–	–	++
TCA15	–	–	–	–
TCA16	–	–	+	–
TCA17	–	–	–	–
TCA18	–	–	–	+
TCA19	+	–	–	++
TCA20	–	–	–	–
TCA21	–	–	–	–
TCA22	–	–	++	–
TCA23	–	–	–	–

–: None; ++: High; +: Low

Pharmacokinetics profiles: Most biomolecules are absorbed through either an active or passive diffusion process. The GI-absorptivity of bimolecular compounds is a vital characteristic to consider. Due to its membrane permeability, the small intestine boasts a larger surface area for drug absorption in the gastrointestinal tract than the stomach [18]. Since the gut is a primary absorption location, it is vital to predict human intestinal absorption of pharmacological molecules [19]. The blood-brain barrier regulates drug molecule access into the brain. Drug-like compounds have the potential to pass the blood-brain barrier and induce hazardous consequences. As a result, it is critical to estimate the compounds' BBB penetrability and toxicity profile [20].

The PGP, like the urine excretion and biliary excretion mechanisms, was critical in the drug disposal process. It is also a crucial element in the oral bioavailability absorption and blood-brain barriers, which restricts drug accumulation in the brain. PGP inhibition induces medication interactions and increases drug accumulation in the brain [21]. Cytochrome P450 is a type of enzyme that is required for drug metabolism. A medication that inhibits cytochrome P450 (CYP) enzymes may reduce drug metabolism and other metabolic processes [22]. The permeability of medicinal compounds to the skin is a significant criterion for the tropical applications. The skin permeation coefficient (KP) measures the rate at which a molecule can penetrate the lipid bilayer membrane of the skin. This metric is expressed in cm/s and is the product of the diffusion coefficient and the thickness of the membrane [23].

Similarly, the results of the aqueous extract are shown in Table-7. The results showed that except molecule TCA-13, all the molecules exhibited GI-absorption capacity. All the molecules except TCA2, TCA9, TCA11, TCA13, TCA14 and TCA22 can cross blood blood-brain barrier (Fig. 4). The ability

TABLE-7
PHARMACOKINETIC POTENTIALS OF SOME MOLECULES ISOLATED FROM AQUEOUS EXTRACT OF *T. cordifolia*

Molecules	GI absorption	BBB permeant	P-gp substrate	CYP1A2 inhibitor	CYP2C19 inhibitor	CYP2C9 inhibitor	CYP2D6 inhibitor	CYP3A4 inhibitor	Log Kp cm/s (skin permeation)
TCA1	H	Y	Y	N	N	N	Y	N	-6.79
TCA2	H	N	N	N	N	N	N	N	-6.31
TCA3	H	Y	N	N	N	Y	N	N	-5.03
TCA4	H	Y	N	Y	N	N	N	N	-5.65
TCA5	H	Y	N	N	N	N	N	N	-6.13
TCA6	H	Y	N	N	N	N	N	N	-5.36
TCA7	H	Y	N	N	N	N	N	N	-5.60
TCA8	H	Y	N	N	N	N	N	N	-6.34
TCA9	H	N	N	N	N	N	N	N	-6.91
TCA10	H	Y	N	Y	N	Y	N	N	-2.77
TCA11	L	N	N	N	N	N	N	N	-7.01
TCA12	H	Y	N	Y	N	Y	N	N	-3.05
TCA13	L	N	N	Y	N	N	N	N	-2.57
TCA14	H	N	Y	N	N	N	N	N	-7.15
TCA15	H	Y	N	N	N	N	N	N	-5.19
TCA16	H	Y	Y	N	N	Y	N	N	-5.76
TCA17	H	Y	Y	N	N	N	N	N	-5.94
TCA18	H	Y	N	N	N	N	N	N	-5.00
TCA19	H	Y	N	Y	Y	Y	N	N	-3.87
TCA20	H	Y	N	N	N	N	N	N	-6.47
TCA21	H	Y	N	N	N	Y	N	Y	-5.21
TCA22	H	N	Y	N	N	N	N	N	-7.58
TCA23	H	Y	N	N	N	N	N	N	-6.14

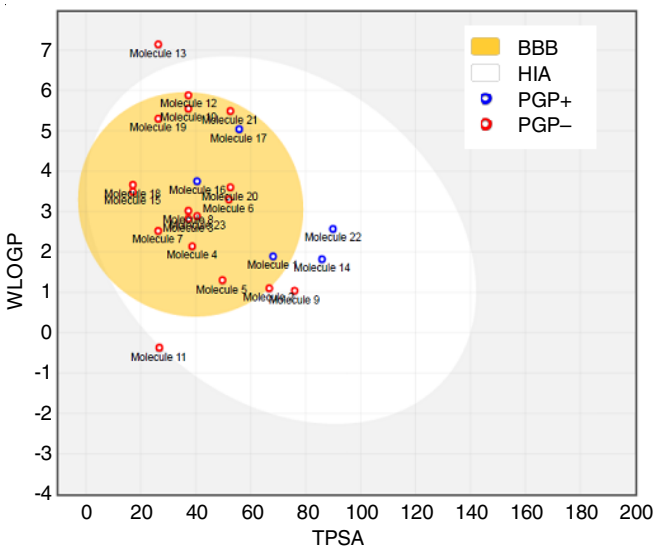

Fig. 4. Boiled egg diagram for the molecule identified in aqueous extract

of human intestine to absorb compounds is more pronounced in molecules TCA9, TCA11, TCA14 and TCA22. Among the compounds studied, molecules TCA1, TCA14, TCA16, TCA17 and TPA22 tended to induce P-glycoprotein (PGP), while the other molecules showed an inclination to inhibit PGP activity. The molecules TCA1, TCA3, TCA4, TCA10, TCA12, TCA13, TCA16, TCA19 and TCA21 inhibit CYP against various CYP inhibitors. The results also showed that the skin permeability of molecules was acceptable.

Docking studies: Initial docking analyses were conducted on various target proteins, including 5zcb, 5ycp and 4pyp, associated with α-glucosidase, PPARγ ligand binding and human glucose transporter GLUT1 inhibition, respectively. Additionally, proteins 1eqg and 3ln1 were considered for evaluating COX-1 and COX-2 inhibitory effects. These analyses encompassed the diverse compounds present in the extract.

Table-8 illustrates the FullFitness (kcal/mol) and binding energy G (kcal/mol) values for aqueous extracts. According to the findings, molecules TCA12, TCA13, TCA21 exhibit high PPARγ ligand binding affinity. Molecules TCA1, TCA12, TCA13 have antidiabetic action through inhibiting GLUT-1. COX1 inhibition is found in molecules TCA10, TCA12, TCA13 and COX2 inhibition is found in molecules TCA10, TCA12, TCA13. Fig. 5 depicted the binding pose and binding residues of molecule TCA12.

Conclusion

In summary, it was found that the aqueous extract of fresh stem of *Tinospora cardifolia* contained the highest quantity of linoleic acid (molecule TCA12). With the exception of molecule TCA4, other compounds revealed in the GC-MS analysis had good toxicity potential, pharmacokinetic profiles and drug likeliness characteristics. Linoleic acid was revealed to have anti diabetic activity due to PPARγ inhibition and strong COX-1 inhibitions. However, from a pharmacological perspective, some development at the formulation level is necessary because of the PGP and CYP-inhibitory impact.

TABLE-8
BINDING ENERGIES OF SOME MOLECULES ISOLATED FROM AQUEOUS EXTRACT OF *T. cordifolia*

Molecule	5ycp		4pyp		1eqg		3ln1	
	FullFitness (kcal/mol)	Binding energy, ΔG (kcal/mol)	FullFitness (kcal/mol)	Binding energy, ΔG (kcal/mol)	FullFitness (kcal/mol)	Binding energy, ΔG (kcal/mol)	FullFitness (kcal/mol)	Binding energy, ΔG (kcal/mol)
TCA1	-1732.4	-7.7	-1143.9	-8.4	-2069.5	-7.5	-2206.3	-7.3
TCA2	-1757.2	-7.9	-1166.1	-7.8	-2100.0	-7.8	-2233.1	-7.4
TCA3	-1822.6	-6.4	-1231.1	-6.5	-2163.6	-6.4	-2299.3	-6.4
TCA4	-1768.9	-6.9	-1176.8	-6.7	-2110.7	-7.2	-2249.9	-7.2
TCA5	-1736.4	-7.2	-1205.8	-6.8	-2139.0	-6.9	-2274.4	-7.1
TCA6	-1795.9	-7.1	-1142.9	-6.9	-2073.9	-6.7	-2209.0	-6.9
TCA7	-1802.2	-6.6	-1207.2	-6.6	-2139.1	-6.4	-2278.4	-6.7
TCA8	-1798.8	-7.3	-1208.3	-7.3	-2133.4	-7.1	-2276.9	-7.2
TCA9	-1788.2	-7.4	-1194.6	-7.1	-2131.4	-7.3	-2269.1	-7.2
TCA10	-1856.1	-8.1	-1270.8	-8.2	-2189.9	-8.2	-2335.0	-8.2
TCA 11	-1804.3	-6.6	-1211.3	-7.1	-2141.8	-6.6	-2279.4	-6.5
TCA 12	-1847.7	-9.3	-1256.2	-8.6	-2183.5	-9.1	-2322.0	-8.6
TCA 13	-1853.6	-8.6	-1262.2	-8.2	-2187.2	-8.9	-2317.6	-8.3
TCA 14	-1735.7	-7.5	-1143.5	-7.4	-2069.0	-6.9	-2208.5	-6.9
TCA 15	-1803.1	-7.5	-1211.4	-6.1	-2144.7	-6.7	-2282.8	-6.7
TCA 16	-1767.3	-7.0	-1178.8	-7.4	-2110.01	-7.3	-2243.1	-7.2
TCA 17	-1772.7	-8.0	-1186.9	-8.4	-2114.1	-7.8	-2236.1	-7.6
TCA 18	-1787.5	-7.0	-1197.3	-6.9	-2127.4	-6.5	-2263.6	-6.6
TCA 19	-1787.6	-7.0	-1198.8	-7.0	-2130.3	-6.4	-2265.8	-6.4
TCA 20	-1787.1	-7.9	-1193.9	-8.1	-2117.3	-7.2	-2250.6	-7.5
TCA 21	1781.2	-8.4	-1184.9	-7.9	-2111.6	-7.6	-2243.5	-7.4
TCA 22	1771.4	-7.9	-1198.2	-8.2	-2112.4	-7.2	-2247.1	-7.3
TCA 23	1811.4	-7.4	-1218.3	-7.1	-2147.2	-7.1	-2291.9	-7.8

Binding energies –6.0 to –7.0 consider as less binding affinity, –7.0 to –8.00 consider as moderate binding affinity and –8.00 to –10.00 consider as good binding affinity.

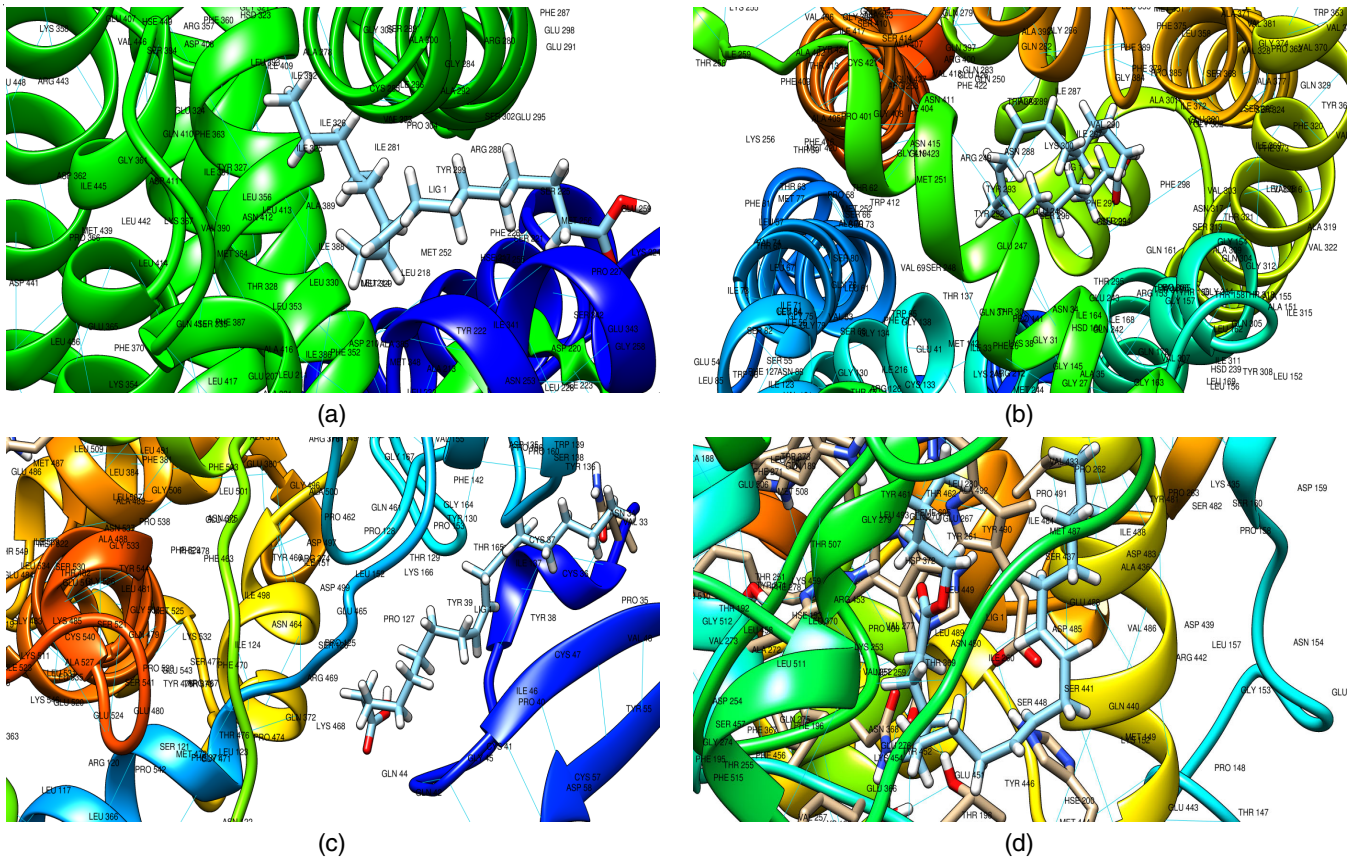

Fig. 5. Binding pose and amino acid residue for molecule TCA12 with 5ycp (a), 4pyp (b), 1eqg (c) and 3In1 (d)

ACKNOWLEDGEMENTS

The authors are grateful to the management of Srikrupa Institute of Pharmaceutical Sciences, Siddipet, India for providing the necessary research facilities. The authors are also thankful to SAIF, IIT Bombay to conduct GC-MS and FTIR analysis.

CONFLICT OF INTEREST

The authors declare that there is no conflict of interests regarding the publication of this article.

REFERENCES

1. V. Anjum, U. Bagale, A. Kadi, I. Potoroko, S.H. Sonawane and A. Anjum, *Molecules*, **28**, 7073 (2023); https://doi.org/10.3390/molecules28207073
2. S. Saha and S. Ghosh, *Ancient Sci. Life*, **31**, 151 (2012); https://doi.org/10.4103/0257-7941.107344
3. N.N. Rege, U.M. Thatte and S.A. Dahanukar, *Phytother. Res.*, **13**, 275 (1999); https://doi.org/10.1002/(SICI)1099-1573(199906)13:4<275::AID-PTR510>3.0.CO;2-S
4. A.K. Upadhyay, K. Kumar, A. Kumar and H.S. Mishra, *Int. J. Ayurveda Res.*, **1**, 112 (2010); https://doi.org/10.4103/0974-7788.64405
5. A. Kumar, A. Voet and K. Zhang, *Curr. Med. Chem.*, **19**, 5128 (2012); https://doi.org/10.2174/092986712803530467
6. B.J. McConkey, V. Sobolev and M. Edelman, *Curr. Sci.*, **83**, 845 (2002).
7. G.R. Marshall, C.D. Barry, H.E. Bosshard, R.A. Dammkoehler and D.A. Dunn, Computer-Assisted Drug Design, ACS Symposium Series **112**, 205 (2019); https://doi.org/10.1021/bk-1979-0112.ch009
8. X.Y. Meng, H.X. Zhang and M. Mezei and M. Cui, *Curr. Computer-Aided Drug Design*, **7**, 146 (2011); https://doi.org/10.2174/157340911795677602
9. S. Sen, B. Ravindar, S. Jala and L. Dharabonia, *Int. J. Pharm. Sci. Res.*, **13**, 3163 (2022); https://doi.org/10.13040/IJPSR.0975-8232.13(8).3163-73
10. P.A. Bafna and R. Balaraman, *Phytomedicine*, **12**, 264 (2005); https://doi.org/10.1016/j.phymed.2003.12.009
11. A. Nicholls, G.B. McGaughey, R.P. Sheridan, A.C. Good, G. Warren, M. Mathieu, S.W. Muchmore, S.P. Brown, J.A. Grant, J.A. Haigh, N. Nevins, A.N. Jain and B. Kelley, *J. Med. Chem.*, **53**, 3862 (2010); https://doi.org/10.1021/jm900818s
12. R. Rohs, I. Bloch, H. Sklenar and Z. Shakked, *Nucleic Acids Res.*, **33**, 7048 (2005); https://doi.org/10.1093/nar/gki1008
13. O. Méndez-Lucio and J.L. Medina-Franco, *Drug Discov. Today*, **22**, 120 (2017); https://doi.org/10.1016/j.drudis.2016.08.009
14. L.Z. Benet, C.M. Hosey, O. Ursu and T.I. Oprea, *Adv. Drug Deliv. Rev.*, **101**, 89 (2016); https://doi.org/10.1016/j.addr.2016.05.007
15. S. Prasanna and R.J. Doerksen, *Curr. Med. Chem.*, **16**, 21 (2009); https://doi.org/10.2174/092986709787002817
16. D. Ji, M. Xua, C.C. Udenigwe and D. Agyeia, *Curr. Res. Food Sci.*, **3**, 41 (2020); https://doi.org/10.1016/j.crfs.2020.03.001
17. A. Husain, A. Ahmad, S.A. Khan, M. Asif, R. Bhutani and F.A. Al-Abbasi, *Saudi Pharm. J.*, **24**, 104 (2016); https://doi.org/10.1016/j.jsps.2015.02.008
18. W.S. Nimmo, *Clin. Pharmacokinet*, **1**, 189 (1976); https://doi.org/10.2165/00003088-197601030-00002
19. M.D. Wessel, P.C. Jurs, J.W. Tolan and S.M. Muskal, *J. Chem. Inf. Comput. Sci.*, **38**, 726 (1998); https://doi.org/10.1021/ci980029a
20. W.M. Pardridge, *J Cereb Blood Flow Metab.*, **32**, 1959 (2012); https://doi.org/10.1038/jcbfm.2012.126
21. Y. Tanigawara, *Ther Drug Monit.*, **22**, 137 (2000); https://doi.org/10.1097/00007691-200002000-00029
22. J.H. Lin and A.Y. Lu, *Clin Pharmacokinet*, **35**, 361 (1998); https://doi.org/10.2165/00003088-199835050-00003
23. R.O. Potts and R.H. Guy, *Pharm Res.*, **9**, 663 (1992); https://doi.org/10.1023/a:1015810312465